The Effect of Magnetic Flux Density on the Performance and Discharge Current Oscillation in a Double-Channel Hall Thruster

By Nanami TAKIGUCHI,[1)] Fuga MATSUO,[1)] Keita NISHII,[1)] and Akira KAKAMI [1)]

[1)] *Tokyo Metropolitan University, Japan*

In recent years, Hall thrusters have gained prominence in electric propulsion systems due to their high anode efficiency, specific impulse, and favorable thrust-to-power ratios. Among the two primary types—Stationary Plasma Thrusters (SPTs) and Thrusters with Anode Layer (TALs)—TALs are considered to offer superior performance and durability. However, their practical deployment has been limited by discharge current oscillations that restrict stable operational ranges and deteriorate variable thrust capability. In this study, a 1.5 kW-class double-channel TAL-type Hall thruster, TMU-D058, was examined to enable a wide variable thrust range by selecting the operating channel. The objective of this study was to elucidate the influence of magnetic flux density and magnetic field distribution on thruster performance and discharge current oscillations. Two comparative experiments were performed: one varying magnetic flux density with fixed magnetic field distribution near the channel exit and the other varying field distribution while keeping flux density constant. The performance variations due to these parameters were not significant. Conversely, increasing the magnetic flux density or modifying the magnetic field configuration effectively suppressed discharge current oscillations in the inner channel. While the double-channel operation suggested the presence of mutual interaction between oscillations, further investigation is necessary to confirm this behavior.

Key Words: Hall thruster, TAL, Magnetic Flux Density, and Discharge current oscillation

Nomenclature

g	:	gravitational acceleration, m/s²
I	:	current, A
I_{sp}	:	specific impulse, s
$\dot{m}$	:	mass flow rate, mg/s
P	:	power, W
T	:	thrust, N
V	:	voltage, V
Δ	:	Oscillation amplitude
η	:	efficiency, %
τ	:	measurement time, s

Subscripts

a	:	anode
d	:	discharge
c	:	coil
i	:	inner
m	:	middle
o	:	outer

1. Introduction

In recent years, the use of electric propulsion systems in spacecraft has been steadily increasing, with Hall thrusters gaining particular attention due to their advantageous characteristics, including relatively high anode efficiency, specific impulse, and thrust-to-power ratio compared to other electric propulsion technologies.[1)] Owing to these advantages, Hall thrusters have been widely employed in both scientific missions and commercial satellite applications.[2)] Structurally, Hall thrusters are classified into two principal types: the Stationary Plasma Thruster (SPT) and the Thruster with Anode Layer (TAL). SPTs feature dielectric insulating walls within the discharge channel, while TALs utilize conducting walls. Although TALs are expected to provide higher performance and longer operational lifetimes than SPTs, their practical use has been hindered by the tendency to exhibit significant discharge current oscillations, resulting in a limited stable operating range.[3)] Consequently, TAL-type thrusters have not yet been deployed in space missions despite their promising performance potential.[4)]

Presently, research is underway to develop Hall thrusters equipped with multiple discharge channels, with the objective of achieving high-power and high-thrust operation. For instance, at the University of Michigan, a nested-channel Hall thruster has been developed in which multiple SPT-type discharge channels are arranged coaxially, as exemplified by the X2 and X3 thrusters with two and three channels, respectively.[5),6)] This architecture offers significant advantages over clustered single-channel configurations, including reduced volume and system complexity. The nested-channel design facilitates variable thrust operation without compromising performance, as each discharge channel can be selectively activated to operate within its optimal conditions—specifically in terms of mass flow rate and discharge voltage—regardless of the overall thrust requirement. In addition to the advantages, this configuration demonstrates a synergistic effect wherein the total thrust produced during the simultaneous operation of multiple channels exceeds the sum of the thrusts generated by individual channels operated independently.

The application of the nested-channel design to TALs, which yielded higher performance than SPTs, would extend variable-thrust range, while maintaining relatively high performance. That is, the appropriate selection of the working discharge channels in accordance with the required thrust would allow both variable thrust range and higher performance.

Hence, we developed a 1.5 kW-class double-channel TAL-type Hall thruster, TMU-D058. Our previous study demonstrated that the nested TAL-type Hall thruster produces stable plasma in single- and double-channel operations. In this study, the thruster was examined with various magnetic flux density distributions to clarify the effect of magnetic flux density distribution on the performance and discharge current oscillation in double-channel operation.

2. Equipment Installation Apparatus

2.1. TMU-D058 Hall thruster

Figure 1 shows a cross-sectional view and picture of TMU-D058. The thruster had discharge channels with inner and outer diameters of 23 mm and 52 mm, respectively. The discharge channel length and width were 6 and 2 mm, respectively. The stainless-steel (SUS316L) guard ring was placed at a distance of 1 mm from the hollow anode made of copper. Four solenoids and screen yokes made of S45C were coaxially placed to apply magnetic fields to the discharge channel. Screen yokes and magnetic poles were made of ferromagnetic steel (S45C) to strengthen the magnetic flux density at the exit of discharge channels. The inner and middle 1 solenoids had 120 and 60 clockwise turns, and the middle 2 and outer solenoids had 60 and 100 counterclockwise turns. The insulators that insulate the anode were made of macerite SP, a highly machinable ceramic. The propellant was supplied into the discharge channel through the supply ports printed by a 3D printer (Formlabs, Form3) using High Temp Resin with a heat resistance of 238 °C and 24 injection holes in the hollow anode. For electron supply, a hollow cathode (MHC1000, Kaufman & Robinson, Inc.) was employed.

Fig. 1. TMU-D058.

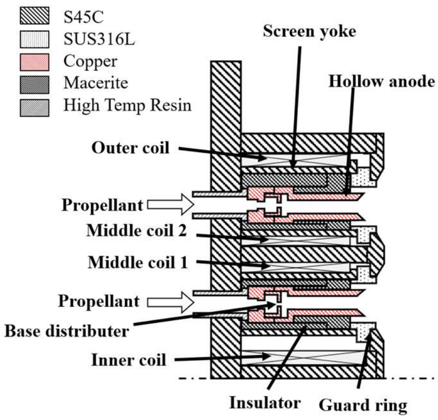

Fig. 2. Axial cross-sectional view of TMU-D058.

2.2. Vacuum chamber (Shinkai 6500)

TMU-D058 was tested in a vacuum chamber (Shinkai 6500), as shown in Fig. 3. The diameter is 1500 mm, and the length is 3200 mm. This vacuum chamber was evacuated with a rotary pump, mechanical booster pump, turbo molecular pump and cryopumps. The ambient pressure was maintained at 1.0×10^{-3} to 10^{-2} Pa during Hall thruster firing. The pressure was measured using an ionization vacuum gauge during the tests.

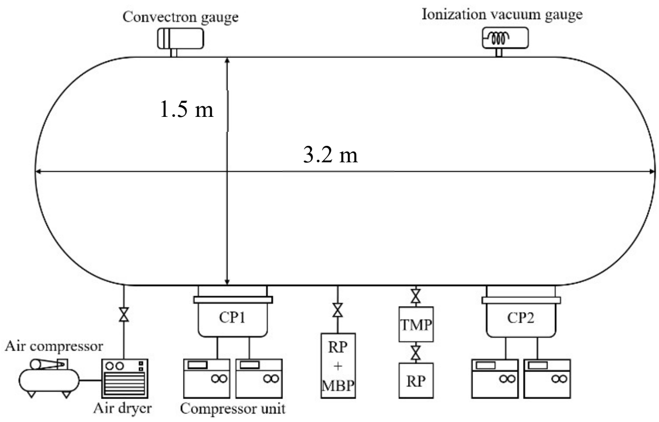

Fig. 3. Vacuum chamber.

2.3. Gas Supply System

Figure 4 shows a schematic of the gas supply system. Xenon was used as a propellant and a working gas of cathode. The Xe gas was decompressed by a regulator and distributed to the inner/outer channels and the hollow cathode. The mass flow rate to the hollow cathode was regulated using two mass flow controllers to extend the mass flow range.

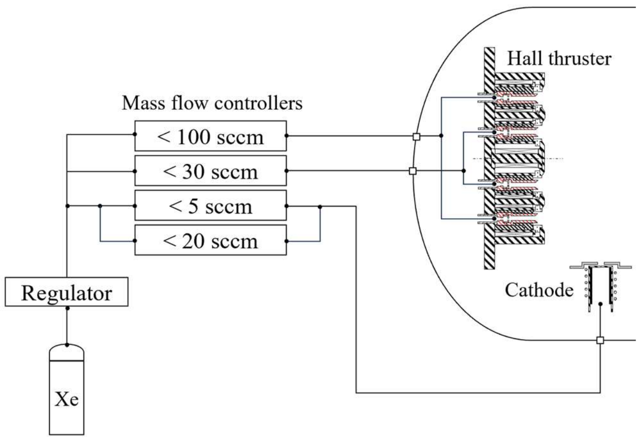

Fig. 4. Schematic of the gas supply system.

2.4. Circuit Configuration and Measurement System

Figure 5 shows a schematic of the Hall thruster driving circuit and measurement system. Two Zener diodes with a breakdown voltage of 51 V were inserted between the cathode and the ground in opposite directions to electrically float the thruster driving circuit. A horizontal pendulum-type thrust stand shown in Fig. 5 was used, and thrust was determined from the output of a laser displacement censor. The discharge current and voltage, and the output of the displacement sensor were recorded with a data logger (Keyence, NR-500 series), and the discharge current was measured using a non-contact current sensor (U-RD, HCS-20-SC-A-05Z-H). The discharge current and backplate current waveforms were measured by an oscilloscope (Rigol, DHO-1104). A hollow cathode was positioned so that its orifice was located 30 mm axially and 60 mm radially from the center of the Hall thruster. A total of five power supplies were utilized: one for the primary discharge of the anode, one each for the inner, middle, and outer coil, and one for the keeper of the cathode, as listed in Table 1.

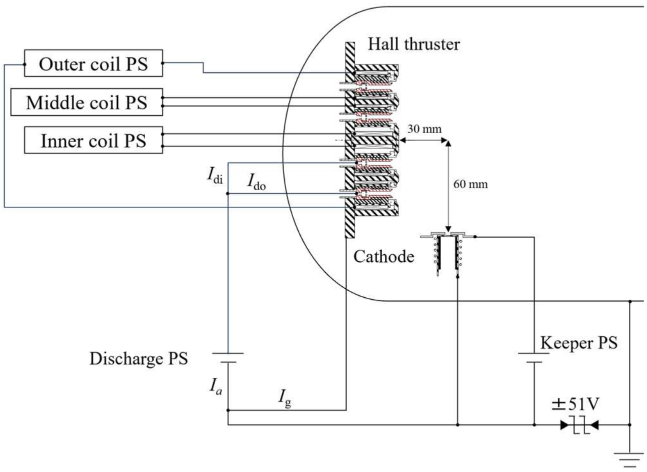

Fig. 5. Circuit configuration.

Table 1. Specifications of power supplies.

	Company	Model	Output, V, A
Discharge PS	TAKASAGO	HX0600-25G	0 - 600, 0 - 25
Inner coil PS	MATSUSADA	PK15-26	0 - 15, 0 - 26
Middle coil PS	RIDEN	RD6012	0 - 60, 0 - 12
Outer coil PS	MATSUSADA	PK80-5	0 - 80 , 0 - 5
Keeper PS	NISTAC	NT-700	0 – 700, 0 - 1

2.7. Performance evaluation

The discharge voltage V_{di} or V_{do} and anode mass flow rate were fixed at 200 V, and the magnetic flux densities at the exit of discharge channels were varied to evaluate performance. The discharge power P_d, Thrust T, Thrust-to-power ratio T/P, specific impulse I_{sp}, and anode efficiency η_a were used to evaluate performance. Equation (1) to (4) were definitions of the performance. The power consumption of solenoids and cathode and the flow rate for the cathode were neglected in the evaluation.

$$P_d = V_d I_d \tag{1}$$

$$\frac{T}{P} = \frac{T}{P_d} \tag{2}$$

$$I_{sp} = \frac{T}{\dot{m}_a g} \tag{3}$$

$$\eta_a = \frac{T^2}{2\dot{m}_a P_d} \tag{4}$$

3. Experimental Conditions

To investigate the effects of magnetic flux density strength and distribution on the performance of a TAL-type double-channel Hall thruster, the currents applied to the inner, middle, and outer coils were varied. Table 2 summarizes the experimental conditions. To clarify the difference in performance for single-channel and dual-channel operations, the discharge voltage was fixed at 200 V, and propellant flow rates for the inner and outer channels were set at 15 and 35 sccm, respectively. Magnetic flux density near the channel exit was adjusted by switching the coil-current conditions #1, #2, and #3. Moreover, the magnetic field distribution was varied with the selection of coil current conditions #1, #4, and #5, while the strength in the inner- and outer-discharge-channel exits was maintained at approximately 25 mT and 35 mT.

Figure 6 illustrates the magnetic field distributions of coil current conditions #1, #4, and #5. Since the ratio of the three coil currents was not modified, the magnetic field distributions in conditions #2 and #3 are equivalent to that in condition #1. Figures 7 and 8 provide magnetic flux density distributions along the centerlines of the inner and outer channels, respectively. The horizontal axis origins are defined as the position of the discharge-channel exit, and the negative values represent the interior of the discharge channel.

Table 2. Experimental condition.

Parameters		Inner channel	Outer channel
Discharge PS voltage, V		200	
Anode mass flow rate, sccm		15	35
Cathode mass flow rate		10 % of Anode mass flow rate	
Back pressure, Pa		1.0×10^{-3} – 8.8×10^{-3}	
Max magnetic flux density, mT	Coil current condition		
	#1	24.6	31.6
	#2	27.5	37.7
	#3	30.1	43.6
	#4	24.2	31.9
	#5	25.0	32.5

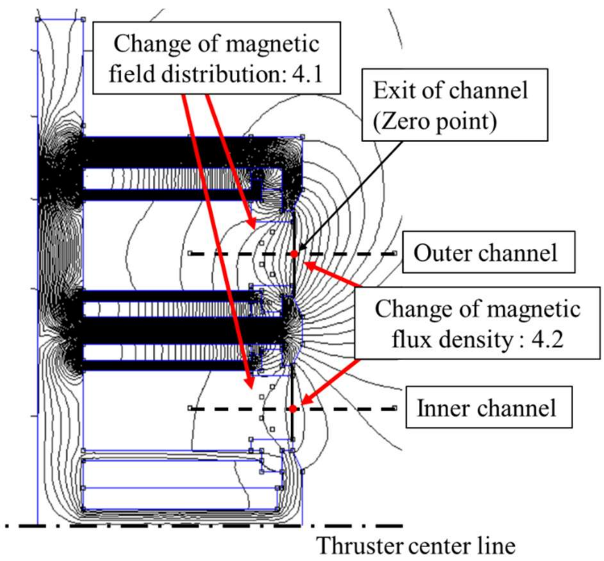

Fig. 6. Changes in magnetic field under various experimental conditions.

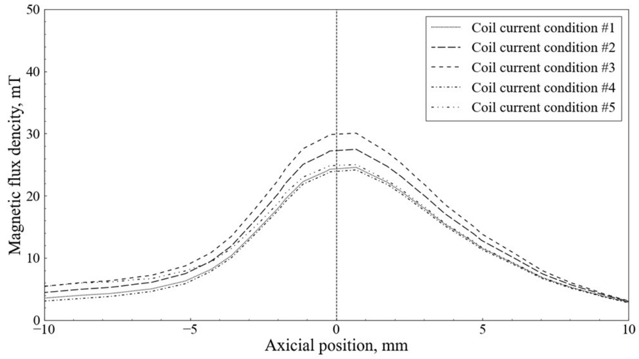

Fig. 7. Magnetic flux density distribution of inner channel.

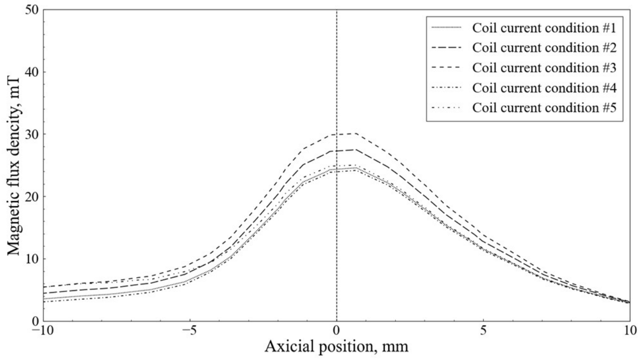

Fig. 8. Magnetic flux density distribution of outer channel.

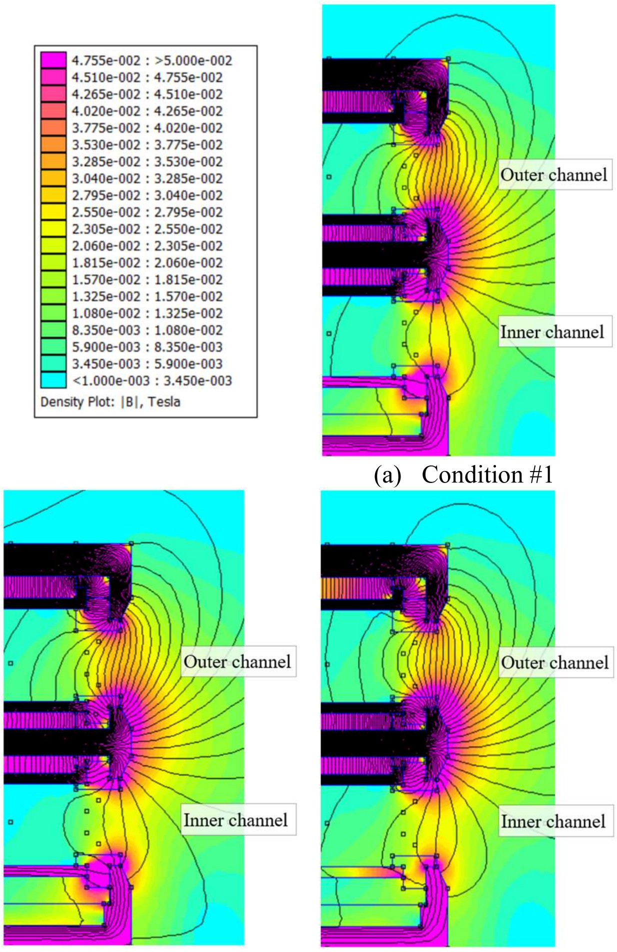

(a) Condition #1

(b) Condition #4 (c) Condition #5

Fig. 9. Magnetic field distribution.

4. Experimental Results and Discussion

In this study, to evaluate the performance of the TMU-D058 Hall thruster, thrust, thrust-to-power ratio, and specific impulse were evaluated under the conditions shown in Table 2, and the effects on discharge current oscillations were also investigated.

4.1 The Effect of Magnetic Flux Density Strength

Figure 10 illustrates the dependence on the strength of the magnetic field density at the discharge channel exit. In inner- and outer-channel operations, a significant reduction in discharge current was observed under coil current condition #3—which had the highest magnetic flux density—compared with condition #1, which had the lowest. The double-channel operation presented a reducing trend in discharge current. Hence, stronger magnetic flux density at the discharge channel exit attenuated discharge current in both single- and double-channel operations.

The thruster presented negligible dependence of magnetic field strength on thrust and specific impulse in both single- and double-channel operations. This dependence was coincident with those for other single-channel thrusters[7].

The thrust-to-power ratio was dependent on the magnetic flux density in outer- and double-channel operations, while keeping constant in the inner-channel operation. This is because, although increasing the magnetic flux density reduced the discharge power, thrust showed significant variation under fewer conditions compared to discharge power. In inner-channel operation, the thrust-to-power ratio differed only under condition #1, where a significant change was observed. Similarly, in double-channel operation, a difference appeared under condition #1, exhibiting the most pronounced augmentation in discharge power when compared to single-channel operation.

The anode efficiency presented the similar trend to that of the thrust-to-power ratio. From these results, the strengthening magnetic flux density reduced discharge current but had negligible effect on performance.

The difference in performance trends depending on the operating mode may be attributed to variations in magnetic flux density strength between the channels. Therefore, under the current conditions, it is not possible to optimize the magnetic flux density for all modes of operation, and it is necessary to further investigate by varying the flux density combinations between the inner and outer channels to identify optimal values.

4.2 The Effect of Magnetic Field Distribution

This section deals with the effect of the magnetic field distribution. Figure 11 illustrates the dependence of performance on the coil current condition. Change in magnetic field flux distribution had a weak influence on discharge current and discharge power, as shown in Figs. 7 and 8. Stronger magnetic flux density at the discharge channel exit seemed to reduce the discharge current.

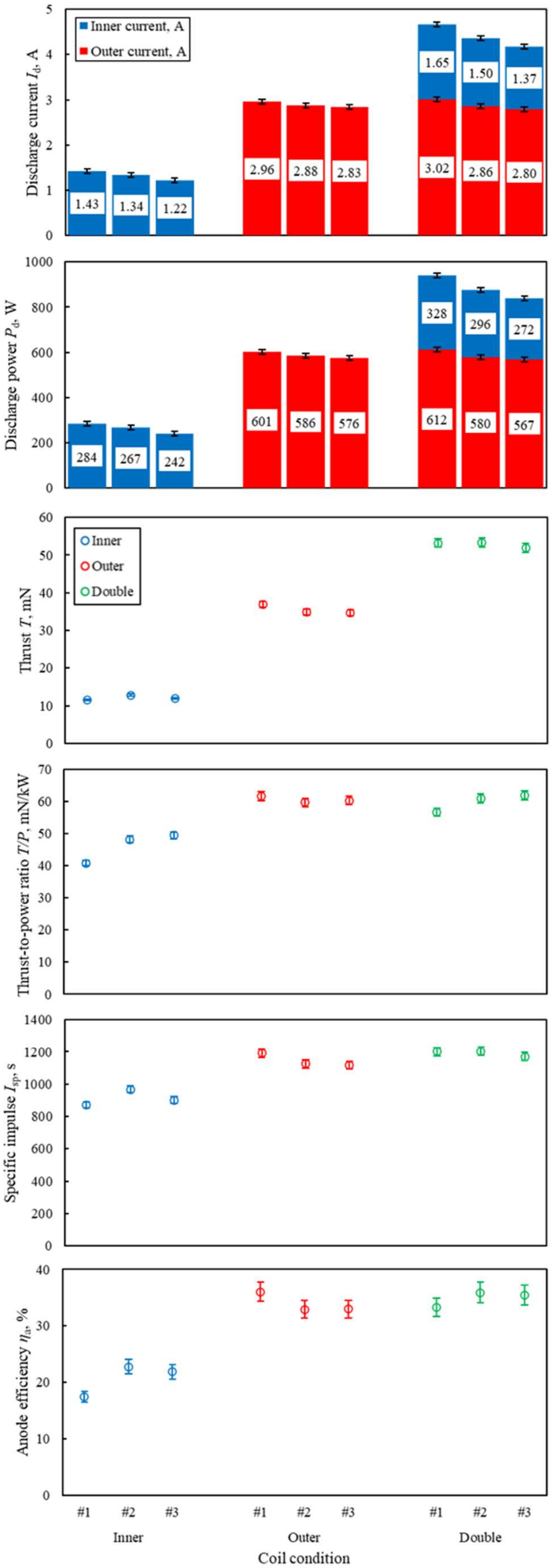

Fig. 10. Performance evaluation with varying magnetic flux density.

In inner- and outer-channel operations, thrust remained effectively unchanged. In outer-channel operation, a change was observed only under condition #4; however, the difference was small. Although the coil current was significantly changed and the magnetic field configuration slightly varied, as shown in Figure 9, the change was not large enough to produce a noticeable impact on performance. Differences in thrust to power ratio, specific impulse, and anode efficiency followed the same trend.

Based on the above results, the following discussion is presented. Generally, a lens-shaped magnetic field near the exit of the discharge channel is considered optimal for Hall thrusters. Under the present experimental conditions, the magnetic field configuration in condition #5 appears to be the most suitable for the outer channel. However, the outer-channel operation did not yield the highest performance under this condition. This is likely because magnetic fields were still present in the non-operating channel even during single-channel operation, allowing electrons from the cathode to leak into the inactive channel.

The presence of magnetic fields in the non-operating channel arises from the system's three-coil design, where generating an appropriate field shape requires current in all coils. Therefore, it is necessary to develop a new thruster design that enables magnetic field generation only in the operating channel, in order to verify this effect. Additionally, in this experiment, the magnetic flux density at each channel exit was kept constant across all conditions to enable a fair comparison. As a result, major changes to the magnetic field configuration were restricted. If both channels could independently generate magnetic fields, it would be possible to more freely vary the magnetic field shapes.

4.3 Discharge Current Oscillations

Figure 12. (a) presents the dependence of normalized discharge current amplitude on the coil current condition., and (b) shows that on magnetic flux density profile with the almost the same magnetic flux density at the discharge channel exit. The normalized discharge-current amplitude (the ratio of discharge current oscillation amplitude to the average) was calculated using the following equation:

$$\Delta = \frac{R.M.S.}{\overline{I_d}} = \frac{1}{\overline{I_d}}\sqrt{\frac{\int_0^{\tau}\left(I_d - \overline{I_d}\right)^2 dt}{\tau}}. \tag{5}$$

Yamamoto et al. defined stable operation as the case with a D ≤0.05, and this definition is used in the paper.[8] Then, in the inner-channel operation, the thruster yielded the stable operation under conditions #2, #3, #4, and #5. As shown in Fig. 12 (a), D was decreased with increasing magnetic flux density. In contrast, the outer channel operation yielded the decreasing trend, but the drop was smaller than the inner channel. From Fig. 12. (b), Δ was smaller in the inner-channel operation under conditions #4 and #5. This indicates that operational stability is affected by not only change in magnetic flux density but also magnetic field distribution. In the outer-channel and double-channel operations, no significant differences in oscillation amplitude were observed.

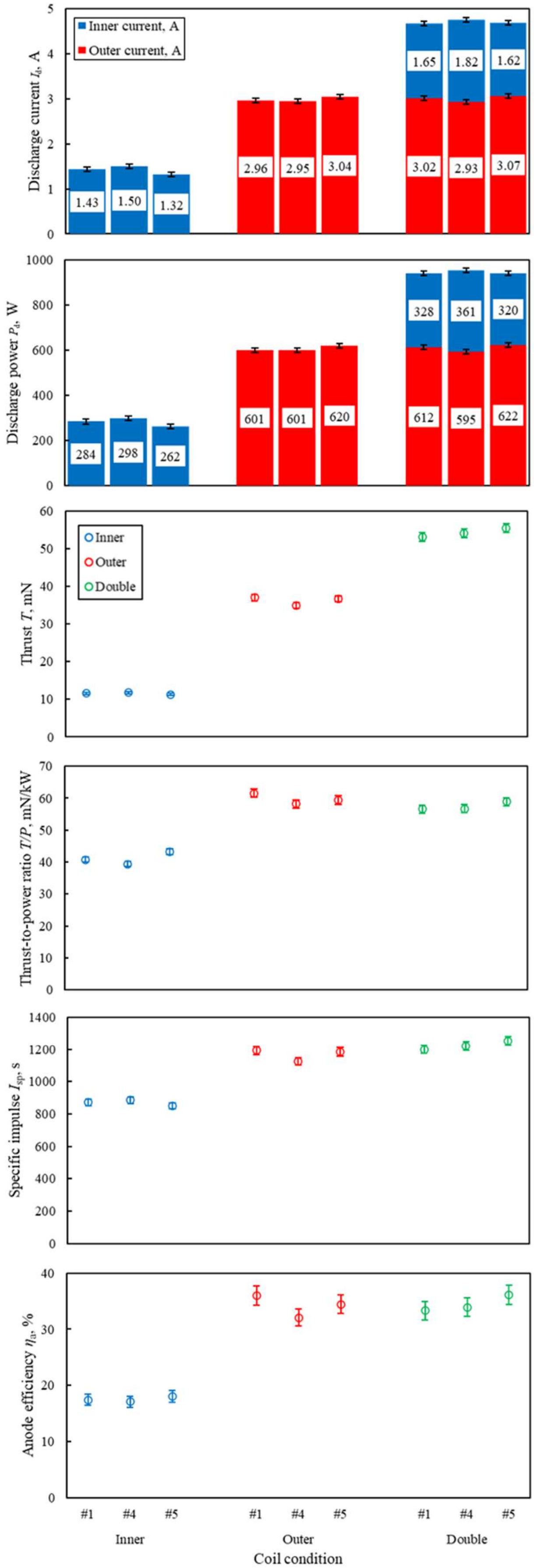

Fig. 11. Performance evaluation with varying magnetic field distribution.

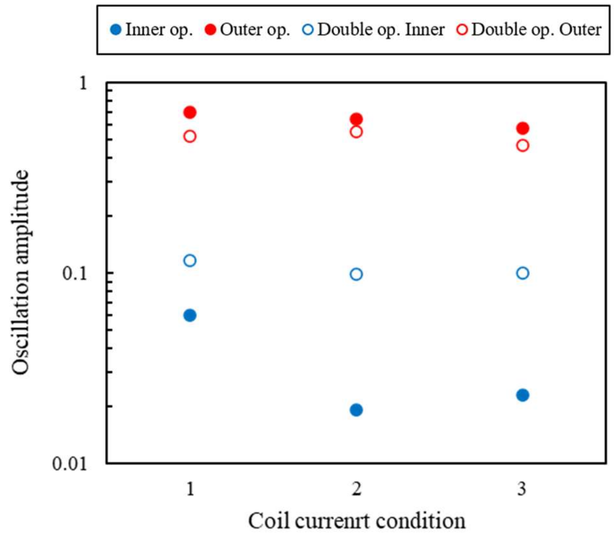

(a)Variation in magnetic flux density.

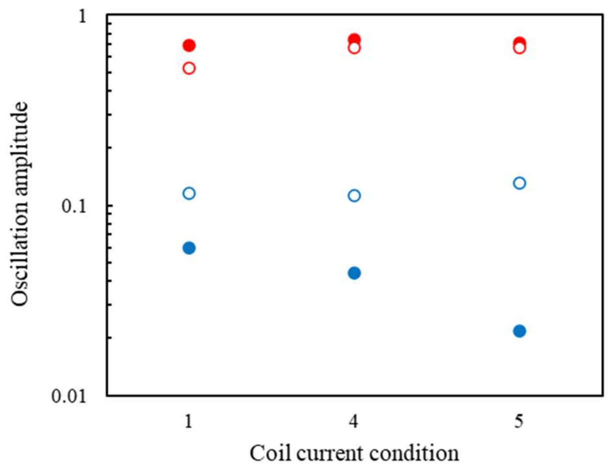

(b)Variation in magnetic field distribution

Fig. 12. Discharge current oscillation amplitude.

When considered collectively, the results from both (a) and (b) reveal the following consistent trend across all conditions. The inner-channel operation demonstrated comparatively higher stability across the range of tested conditions, while the outer-channel operation exhibited the greatest instability. In the context of double-channel operation, the inner channel exhibited a decline in stability relative to its performance under single-channel operation. Conversely, the outer channel demonstrated a modest enhancement in stability. The significant increase in the oscillation amplitude of the inner channel suggests that it was strongly affected by the outer channel. One potential cause of inter-channel interaction during double-channel operation is the shared use of the anode power supply. It will be necessary to verify this by supplying separate anode power sources to each channel. Furthermore, the oscillation amplitude in the outer channel exhibited minimal dependence on magnetic flux density or magnetic field configuration, suggesting that stability enhancements may necessitate adjustments to other parameters, such as discharge voltage or propellant mass flow rate. Therefore, in order to achieve stable double-channel operation, it is necessary to stabilize the outer channel using approaches other than magnetic flux density or field configuration.

5. Conclusion

The performance of a double-channel TAL-type Hall thruster, TMU-D058, was evaluated with magnetic flux density and magnetic field distribution.

Increasing the magnetic flux density led to a decrease in discharge current. Nevertheless, the change in performance trends was minimal. The alteration of the magnetic field configuration did not result in significant performance differences, likely because the changes were constrained in order to maintain the same magnetic flux density at the channel exits. The discharge current oscillation amplitude generally decreased with increasing magnetic flux density. Furthermore, within the inner channel, a reduction in oscillation amplitude was observed through modification of the magnetic field configuration without an increase in magnetic flux density. The influence on the outer channel was negligible in terms of both magnetic flux density and distribution. In double-channel operation, the amplitude of the inner channel was found to be greater than that observed during single-channel operation. This indicates that the inner channel oscillation may be influenced by the outer channel, which demonstrated a higher amplitude.

In the TMU-D058, a magnetic field is generated even in the non-operating channel during single-channel operation, which may influence the performance and discharge current oscillations. Moreover, the restricted flexibility in coil current combinations impedes the ability to fully assess the effects of magnetic field distribution. Consequently, it is imperative to design and evaluate a thruster capable of generating independent magnetic fields for each channel in subsequent studies.

Acknowledgements

This research was supported by JKA through its promotion funds from KEIRIN RACE (No. 2025M-523).

References

1) Dan M. Goebel and Ira Katz.: *Fundamentals of Electric Propulsion: Ion and Hall Thrusters*, Jet Propulsion Laboratory California Institute of Technology, 2008, pp. 325–329.
2) D. Leva, R. M. Myersb, K. M. Lemmerc, J. Kolbeckd, H. Koizumi and K. Polzinf,: The technological and commercial expansion of electric propulsion, *Acta Astronautica,* Vol.159, 2019, pp.213-227.
3) J. M. Sankovic, T. W. Haag and D. H. Manzella.: Operationg Characteristics of the Russian D-55 Thruster with Anode Layer, NASA Technical Memorandam 106610, AIAA-94-3011, pp.1-21.
4) N. Yamamoto, S. Momo, K. Komurasaki, Y. Arakawa.: Discharge Current Oscillations in Hall Thrusters", ISTS 2000-b-23, pp.1-6.
5) Raymond Liang and Alec D. Gallimore.: Constant-Power Performance and Plume Measurements of a Nested-Channel Hall-effect Thruster, 32nd International Electric Propulsion Conference, Wiesbaden, Germany, IEPC-2011-049, 2011.
6) Scott J. Hall, Benjamin A. Jorns, Alec D. Gallimore, Hani Kamhawi, Thomas W. Haag, Jonathan A. Mackey, James H. Gilland, Peter Y. Peterson and Matthew J. Baird.: High-Power Performance of a 100-kW Class Nested Hall Thruster, 35th International Electric Propulsion Conference, Atlanta, Georgia, USA, IEPC-2017-228, 2017.
7) N. Yamamoto, K. Komurasaki and Y. Arakawa.: Discharge Current Oscillation in Hall Thrusters, Jornal of Propulsion and Power, Vol. 21, No. 5, 2005.
8) N. Yamamoto, T. Nakagawa, K. Komurasaki, Y. Arakawa.: Discharge plasma fluctuations in hall thrusters, *Vacuum* 65 (3-4) (2002) 375–381.